Quantification of interaction and topological parameters of polyisoprene star polymers under good solvent conditions

Durgesh K. Rai,[1,*] Gregory Beaucage,[2,†] Kedar Ratkanthwar,[3,4] Peter Beaucage,[5]
Ramnath Ramachandran,[6] and Nikos Hadjichristidis[4]

[1]*Biology and Soft Matter Division, Oak Ridge National Laboratory, P.O. Box 2008, MS-6454 Oak Ridge, Tennessee 37831, USA*
[2]*Materials Science and Engineering, University of Cincinnati, 492 Rhodes Hall, Cincinnati, Ohio 45221, USA*
[3]*Department of Chemistry, University of Athens, Panepistimiopolis, Zografou 15771, Athens, Greece*
[4]*KAUST Catalysis Center, Division of Physical Sciences and Engineering, King Abdullah University of Science and Technology (KAUST), Thuwal, Saudi Arabia*
[5]*Department of Materials Science and Engineering, Cornell University, Ithaca, New York 14853, USA*
[6]*Procter & Gamble, 1 P&G Plaza, Cincinnati, Ohio 45202, USA*

(Received 18 January 2016; published 5 May 2016)

Mass fractal scaling, reflected in the mass fractal dimension d_f, is independently impacted by topology, reflected in the connectivity dimension c, and by tortuosity, reflected in the minimum dimension $d_{\min}$. The mass fractal dimension is related to these other dimensions by $d_f = cd_{\min}$. Branched fractal structures have a higher mass fractal dimension compared to linear structures due to a higher c, and extended structures have a lower dimension compared to convoluted self-avoiding and Gaussian walks due to a lower $d_{\min}$. It is found, in this work, that macromolecules in thermodynamic equilibrium display a fixed mass fractal dimension d_f under good solvent conditions, regardless of chain topology. These equilibrium structures accommodate changes in chain topology such as branching c by a decrease in chain tortuosity $d_{\min}$. Symmetric star polymers are used to understand the structure of complex macromolecular topologies. A recently published hybrid Unified scattering function accounts for interarm correlations in symmetric star polymers along with polymer-solvent interaction for chains of arbitrary scaling dimension. Dilute solutions of linear, three-arm and six-arm polyisoprene stars are studied under good solvent conditions in deuterated p-xylene. Reduced chain tortuosity can be viewed as steric straightening of the arms. Steric effects for star topologies are quantified, and it is found that steric straightening of arms is more significant for lower-molecular-weight arms. The observation of constant d_f is explained through a modification of Flory-Krigbaum theory for branched polymers.

DOI: 10.1103/PhysRevE.93.052501

I. INTRODUCTION

The physical properties of branched polymers are different from linear chains of comparable molecular weight [1–3]. Amongst various possible branched architectures, symmetric star polymers are one of the simplest topologies and have been widely studied from the perspective of synthesis, structure, properties, and application [4–8]. Star polymers are branched macromolecules with all branches or "arms" emanating from a core. The presence of structural constraints, owing to the presence of a common branch point, leads to differences in chain conformation and thermodynamics in star polymers compared to their linear counterparts [9–15]. Moreover, the number and structure of arms have been found to have direct consequences on rheological properties of branched polymers [16–18].

Zimm and Stockmayer (ZS) evaluated the radius of gyration R_g^{star}, of a star polymer with f arms in dilute solution assuming that intra- and interarm spacings follow Gaussian statistics [11,12],

$$R_g^{\text{star}} = R_g^{\text{arm}} \left(\frac{3f-2}{f} \right)^{1/2}, \tag{1}$$

where R_g^{arm} is the radius of gyration of a Gaussian linear chain in dilute solution with the mass of one arm. A notable result inferred from Eq. (1) is that the ratio $R_g^{\text{star}}/R_g^{\text{arm}}$ has a maximum limiting magnitude of $\sqrt{3}$ as $f \to \infty$ under a Gaussian assumption. This result is rather meaningless since steric constraints would render the arms highly non-Gaussian at high f. Moreover, the results from the Gaussian approximation for stars may not hold under virtually any conditions since the intramolecular excluded volume becomes more significant due to increase in segment-segment interactions near the branch point and the Gaussian assumption fails to recognize the singular nature of the branch point [19]. For stars with higher functionality, the arms of the star might behave as stiff chains with a limiting conformation of rigid straight arms for very high f. Assuming a limiting rigid straight-arm configuration for stars, $R_g^{\text{star}}/R_g^{\text{arm}} \sim \sqrt{z_{\text{arm}}}$, for $f \to \infty$, where z_{arm} is the mass associated with each arm and R_g^{arm} is assumed to be Gaussian. This is significantly larger than the prediction of Eq. (1) at large f.

Daoud and Cotton (DC) and later Birshtein and Zhulina addressed the issue of minimization of the free energy due to intermolecular interactions by generalizing the de Gennes's scaling (blob) model for star polymers [12–14,20]. The interarm repulsive interaction was minimized by assuming that equal segments of the arms are confined to growing spherical blobs that can fit into a cone as the arms extend away from the branch point (core). The star polymer adopts a conformation

*raidk@ornl.gov, raidurgesh@hotmail.com
†beaucag@uc.edu, gbeaucage@gmail.com

in which each of the f arms is constrained within a cone of solid angle $4\pi/f$ radiating from the branch point, which leads to increases in the mean separation between the arms with the distance from the center [13,19]. As per the DC model, the star polymer is confined to shells of decreasing chain density. There is no scattering function associated with the DC model so it is difficult to directly verify this structural model. Under another widely used theory for the star polymers, the chain structure does not display core-shell morphology but it rather acquires a uniform chain density as per Benoit's model for star polymers [21,22]. The Benoit model assumes Gaussian conformation consistent with the Zimm and Stockmayer model but allows for interarm correlations that have been experimentally verified.

The Daoud and Cotton model describes the conformation of a star polymer with f arms with l and v as the monomer length and excluded volume [13,14,20]. According to the DC model, a star polymer has a solid core of radius $r_2 \sim f^{1/2}l$, where the monomer concentration $\phi(r)$ is constant since $\phi(r) \sim M/V$ and for a three-dimensional solid $M \sim (r/l)^3$ and $V \sim (r/l)^3$. Thereafter, $\phi(r)$ varies as $(r/l)^{-1}$ between r_2 and r_1 which fits Gaussian scaling since for a Gaussian chains $M \sim (r/l)^2$ and $V \sim (r/l)^3$, leading to $\phi(r) \sim (r/l)^{-1}$, where $r_1 \sim f^{1/2}v^{-1}l$. Finally, $\phi(r) \sim (r/l)^{-4/3}$ for $r > r_1$, which suggests good solvent scaling for larger distances from the core since for a chain under good solvent conditions $M \sim (r/l)^{5/3}$ and $V \sim (r/l)^3$, leading to $\phi(r) \sim (r/l)^{-4/3}$. The modified Flory-Krigbaum model, presented below, predicts that $\phi(r) \sim (r/l)^{-4/3}$ irrespective of distance from the core, similar to the Zimm-Stockmayer and Benoit models [11,21], with packing constraints accommodated by straightening out of the arms near the core. The Kuhn unit density is constant with good solvent scaling throughout the star. The model follows the same scaling laws as the large-distance prediction of the DC model.

For the "swollen region" [13] of the star, the DC model predicts

$$R \sim f^{1/5}\left(\frac{z}{f}\right)^{3/5} V_C^{1/5} l_k \sim f^{-2/5} z^{3/5} V_C^{1/5} l_k, \qquad (2)$$

where R is the chain end-to-end distance and V_C is the excluded volume per Kuhn unit of length l_k. $z = f z_{\mathrm{arm}}$ is the total mass associated with all the f arms of the star polymer. On the other hand, for the "unswollen" region,

$$R \sim f^{1/4}\left(\frac{z}{f}\right)^{1/2} l_k \sim f^{-1/4} z^{1/2} l_k. \qquad (3)$$

For comparison, using Zimm and Stockmayer's Eq. (1), Orofino predicts the size of symmetric star polymers to be [11,23,24],

$$R \sim \left(\frac{3f-2}{f}\right)^{1/2}\left(\frac{z}{f}\right)^{1/2} l_k \sim \frac{(3f-2)^{1/2}}{f} z^{1/2} l_k \qquad (4)$$

for θ solvent conditions.

Modification of the Flory-Krigbaum model for star polymers

Flory and Krigbaum [25–27] predicted that the expected mass fractal dimension for a linear chain ($c = 1$, defined below) in a good solvent is 5/3 ($d_{\min} = d_f = 5/3$, defined below). This is obtained by modification of the Gaussian chain probability function by a term reflecting self-avoidance, resulting in the expression

$$W(R) = kR^2 \exp\left(-\frac{3R^2}{2zl_k^2} - \frac{z^2 V_C}{2R^3}\right), \qquad (5)$$

where k is a constant. The first term describes Gaussian scaling and the second term reflects the excluded volume by considering the probability of one Kuhn unit being excluded by one of the other Kuhn units of the chain. Assuming that, due to symmetry, a linear chain of length $2z/f$ has the same size as a star of mass z if the two structures have the same degree of tortuosity reflected in $d_{\min}$, $(2z/f)$ is substituted for z in Eq. (5). In the symmetric star, V_C from a linear chain of length $2z/f$ is amplified by f. So fV_C substitutes for V_C,

$$W(R) = kR^2 \exp\left(-\frac{3fR^2}{4zl_k^2} - \frac{(2z/f)^2 f V_C}{2R^3}\right)$$
$$= kR^2 \exp\left(-\frac{3fR^2}{4zl_k^2} - \frac{2z^2 V_C}{fR^3}\right) \qquad (6)$$

Equation (5) can be minimized to find the most likely chain end-to-end distance R^*, ignoring higher-order terms,

$$R^* = R_0^*\left(\frac{2z^{1/2}V_C}{l_k^3}\right)^{1/5} = kz^{3/5}V_C^{1/5}l_k^{2/5}. \qquad (7)$$

A similar minimization of Eq. (6) yields

$$R^* = k\left(\frac{z}{f}\right)^{3/5}(fV_C)^{1/5}l_k^{2/5} = kf^{-2/5}z^{3/5}V_C^{1/5}l_k^{2/5}. \qquad (8)$$

Equation (8) predicts that d_f is independent of f since $R^* \sim z^{1/d_f}$, and that $d_f = 5/3$ for macromolecules in good solvents regardless of topology. Equation (8) also predicts a dependence on functionality similar to that of the DC model described by Eq. (2). It is expected that Gaussian chains will display a mass fractal dimension of 2 regardless of chain topology, as assumed by the DC and Zimm and Stockmayer models. For chains with a fixed mass fractal dimension and variable branch content, the connectivity dimension will increase with branching, and since $d_{\min} = d_f/c$, a reduction in $d_{\min}$ and straightening out of the star arms is expected, as discussed below. Table I shows the three predictions for chain size from the ZS, DC, and modified FK models.

II. SCALING MODEL FOR SYMMETRIC STAR POLYMERS

In this paper, a recently proposed model to analyze scattering from star polymers is used based on a scaling

TABLE I. Summary of R dependence on scaling parameters, f, z, l_k, and V_C.

Model	Theta solvent	Good solvent
Zimm-Stockmeyer	$\frac{(3f-2)}{f}^{1/2} z^{1/2} l_k$	–
Daoud-Cotton	$f^{-1/4} z^{1/2} l_k$	$f^{-2/5} z^{3/5} V_c{}^{1/5} l_k$
Modified Flory-Krigbaum	$\frac{(3f-2)}{f}^{1/2} z^{1/2} l_k$	$f^{-2/5} z^{3/5} V_C{}^{1/5} l_k^{2/5}$

model that allows for study of steric chain extension as well as accounting for polymer-solvent interactions. The scaling approach quantifies the topological as well as thermodynamic parameters for different molecular weights for their linear, three-arm, and six-arm polyisoprene stars under good solvent condition at 34.5 °C in deuterated p-xylene [28].

In the scaling model a macromolecular chain composed of z Kuhn units of length l_k [29] is considered. Figure 1 shows a six-arm symmetric star polymer. The structure displays tortuosity in the chain path associated with a competition between thermal randomization of the chain structure, chain continuity, and steric constraints. The structure also displays topological connectivity that is independent of these thermodynamic and steric constraints. These features can be distinguished by considering the average minimum path of p Kuhn units through the structure [30–32]. One possible minimum path is shown in units with dark borders in Fig. 1. In addition to an average minimum path, an average connectivity path of s Kuhn units composed of straight lines connecting the branch point and chain end points is considered as shown by solid black lines in Fig. 1. In the case of symmetric star polymers, the minimum path is composed of two arms of the star polymer (dark units in Fig. 1). For a symmetric star polymer, the average minimum path p is given by

$$p = 2\left(\frac{z}{f}\right). \tag{9}$$

In general, the minimum path p is related to the mass z through the connectivity dimension c, which represents the mass fractal dimension for the connectivity path. On the other hand, the connectivity path of s is related to the mass through the minimum dimension $d_{\min}$, which represents the mass fractal dimension for the minimum path. Two pairs, $s : d_{\min}$ and $p : c$, work in tandem to represent the whole structure as a mutually conjugate set of parameters such that the mass z can

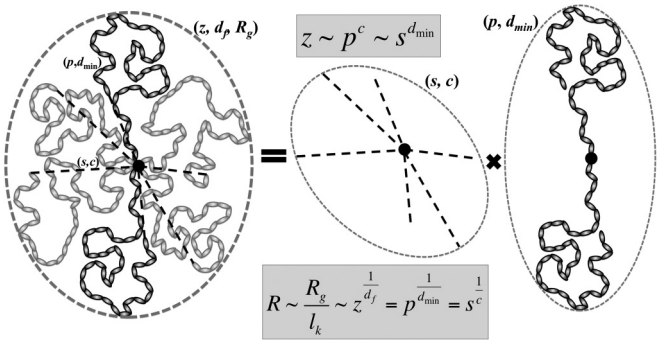

FIG. 1. Schematic of a six-arm PI star polymer of fractal dimension d_f and composed of z Kuhn units of length l_k. The structure can be decomposed into two sets of conjugate parameters describing connectivity (s,c) and tortuosity (p,$d_{\min}$). The connective path is composed of s units and has its nascent fractal dimension called the connective dimension c; and describes the branching characteristics in the chain, shown in straight black dashed lines. Any two branches of a symmetric star form a minimum path across the whole structure composed of p Kuhn units with a nascent fractal dimension called the minimum dimension of $d_{\min}$. p describes the average topological tortuosity and is shown in units with dark borders.

be obtained by raising the connectivity path, s to the minimum dimension $d_{\min}$, or alternatively raising the minimum path p to the topological connectivity dimension c, giving, [31,33,34]

$$z = p^c = s^{d_{\min}}. \tag{10}$$

The connectivity dimension c quantifies the structural connections between the various arms of the polymer and is related to the fractal dimension d_f by [31]

$$d_f = c d_{\min}. \tag{11}$$

c increases with increased branching or connectivity, while d_f increases with tortuosity in the chain. For a linear polymer chain, $d_{\min} = d_f$ and $c = 1$, while, for a completely connected regular object like a sphere or a collapsed coil, $d_f = c$ and $d_{\min} = 1$, since the minimum path becomes a straight line across the whole mass. For a chain under good solvent conditions, $d_{\min} = 5/3$ [31].

For symmetric stars, the mole fraction branch content (ϕ_{Br}) is given by [31]

$$\phi_{\mathrm{Br}} = \frac{(z-p)}{z} = 1 - z^{-(1-1/c)} = \frac{(f-2)}{f}, \tag{12}$$

where $(z - p)$ represents the mass of the coil that does not lie on the minimum path. Further, the connectivity dimension c may be evaluated for symmetric stars from Eq. (12) as [28]

$$c = \frac{\ln z}{\left\{\ln z + \ln\left(\frac{2}{f}\right)\right\}}. \tag{13}$$

A "meandering" mole fraction (ϕ_M) can be defined as the fraction that accounts for mass that is not used in direct or linear connectivity [28],

$$\phi_M = \frac{(z-s)}{z} = 1 - z^{-(1-1/d_{\min})}. \tag{14}$$

As the functionality f increases, $d_{\min}$ and ϕ_M are expected to decrease since steric constraints on the chain conformation increase in comparison to linear chains. For linear chains in the absence of steric effects, ideal scaling behavior is expected. For a good solvent, $d_{\min} \approx 5/3$. Steric interactions between arms in a star have the effect of extending the star arms towards $d_{\min} \to 1$ for a fully extended chain. The limits of an unperturbed (linear) chain and a fully extended chain can be used to define a measure of steric interaction between the arms of a star as [28,35]

$$\phi_{\mathrm{Si}} = \frac{\langle \Delta s \rangle_f}{\langle \Delta s \rangle_\infty} = \frac{s_f - s_{\mathrm{linear}}}{s_\infty - s_{\mathrm{linear}}} = \frac{z^{1/d_{\min}} - z^{1/d_{f,l}}}{z - z^{1/d_{f,l}}}, \tag{15}$$

where $d_{f,l}$ is the fractal dimension of an unperturbed arm under the given solvation conditions [28] and therefore, $d_{f,l} \sim 5/3$ under good solvent conditions, and 2 under theta solvent conditions. ϕ_{Si} is a unique quantitative measure of steric effects in stars (extendible to any branched structure). For star polymers, ϕ_{Si} is the ratio of the extra extension $\langle \Delta s \rangle_f$ in an arm induced due to the presence of other connected arms in the chain to that of the maximum possible extension under the condition $f \to \infty$, $\langle \Delta s \rangle_\infty$. It provides a quantitative measure

of the extension of an arm induced due to the presence of other arms in the chain. In the absence of other branches, i.e., for linear chains, ϕ_{Si} is zero while it is maximum at 1, for a star with straight arms.

A. Scattering functions for star polymers

Small-angle scattering can be used to quantify the scaling model parameters [28,31,36–38]. For macromolecules in dilute solution, contrast enhancement is often achieved by examining hydrogen polymers in deuterated solvents using neutron scattering (SANS).

In order to examine stars under good solvent conditions, a fractal model by Teixeira *et al.* [39] has been employed [40], which is based on the pair correlation function [41],

$$g(r) \sim r^{d_f-3} e^{-r/\xi}. \tag{16}$$

This pair correlation function takes advantage of the simple Fourier transform of a fractal scattering power law for the first term. The problem with this transform is that it reaches infinity at $r = 0$ making the inverse transform impossible. Since there is no basis to "cut off" the power-law term at low r, an *ad hoc* approach is introduced. In Eq. (2), r is the distance between chain units, d_f is the fractal dimension, and ξ is defined as the fractal correlation length which is an artificially introduced size scale for the *ad hoc* exponential cutoff term in Eq. (16). This exponential term was proposed by Debye and Bueche when they observed the scattering profile of blue light by Lucite [42]. Debye and Bueche treated $g(r)$ in a similar way to Debye's charge screening function parametrized by the screening length. They introduced an exponential cutoff function as an "example" after defining ξ as a "kind" of correlation length, in direct analogy to a screening length [42]. Equation (16) is used to obtain the scattered intensity given by Teixeira *et al.* [39],

$$I(q) = 1 + \frac{1}{(qR_m)^{d_f}} \frac{d_f \Gamma(d_f-1)}{\{1+(q\xi)^{-2}\}^{(d_f-1)/2}} \times \sin\{(d_f-1)\tan^{-1}(q\xi)\}, \tag{17}$$

where, $q = (4\pi/\lambda)\sin(\theta/2)$, is the scattering wave vector for a radiation of wavelength λ and R_m is the mean radius of the particle. Equations (16) and (17) are based on the *ad hoc* exponential cutoff term $e^{-r/\xi}$, which was an empirical proposition of Debye and Bueche [42]. The exponential function has no connection to physical structure and the length scale ξ lacks physical meaning.

Benoit evaluated intensity for a star poymer with f arms by modifying Debye's scattering function for a Gaussian polymer chain to account for interarm interactions [21,22,43],

$$\langle I(q)\rangle \approx \frac{2}{fx^2}\left[\{x-(1-e^{-x})\} + \frac{f-1}{2}\{(1-e^{-x})^2\}\right] \tag{18}$$

with $x = f/(3f-2)q^2\langle R^2_{g_{arm}}\rangle$, where $\langle R^2_{g_{arm}}\rangle$ is the Gaussian mean squared radius of gyration of an arm. Equation (18) includes two terms in the main bracket, the first of which reflects scattering from the f arms as individual Gaussian chains, $I_1(q) \approx (2/fx^2)\{x-(1-e^{-x})\}$ and is similar to Debye's scattering function for linear chains. This term dominates the scattering at very high q. The second term in the main bracket, $I_2(q) \approx [(f-1)/fx^2]\{(1-e^{-x})^2\}$, reflects interference between chain units on different arms of the star polymer and dominates the scattering at intermediate and low q but imparts negligible contribution to the scattered intensity at high q. Therefore Eq. (18) predicts a slope of -2 at high q associated with a Gaussian chain. This is consistent with the modification of the Flory-Krigbaum theory presented above for star polymers and the Zimm-Stockmayer prediction for star size. The Benoit model is a fractal model with constant chain scaling, that is, it does not agree with the DC model. For Gaussian stars the Benoit model has been widely used to model scattering data.

B. Hybrid Unified Fit function

Generally, SANS data from a dilute polymer solution displays two structural levels [28,32,35]. In each structural level, a Guinier law $I(q) \sim G\exp(-q^2R_g^2/3)$ and a power law $I(q) \sim B_f q^{-d_f}$ are observed at lower and higher q values, respectively, where G, R_g, B_f, and d_f are the Guinier law prefactor, radius of gyration, power-law prefactor, and fractal dimension ($1 \leqslant d_f \leqslant 3$), respectively. Together, these laws give an account of local features like size (R_g and persistence length $l_p = l_k/2$) and mass fractal dimension. However, in star polymers, owing to the common branch point for the arms, Benoit found that another set of Guinier and power laws are induced due to interarm interactions [21]. This has been experimentally demonstrated. In addition to these structural parameters, the Flory interaction parameter χ can be quantified using the random phase approximation (RPA) equation, accounting for the enthalpy of mixing for a polymer in solution. Taking into account these interactions in the star polymer under dilute solvent conditions, Rai *et al.* obtained [28]

$$\frac{1}{I(q)} = \frac{1}{G_f}\left(\left[\begin{array}{l}\frac{f-1}{2}\left\{e^{-(qR_g)^2/3} + \frac{d_{\min}^2\Gamma(d_f-1)}{R_g^{2d_f}}e^{-(ql_p)^2/9}(q_f^*)^{-2d_f}\right\} \\ +\left\{e^{-(qR_g)^2/3} + K_f e^{-(ql_p)^2/9}(q_f^*)^{-d_f}\right\} + \frac{1}{z}\left\{e^{-(ql_p)^2} + zK_p(q_p^*)^{-1}\right\}\end{array}\right]^{-1} + z\phi K_v\left(1-\frac{2\chi}{\sqrt{K_v}}\right)\right), \tag{19}$$

where Γ is the Gamma function, $q_i^* = q/\{\mathrm{erf}(qk_{sc}R_{g,i}/\sqrt{6})\}^3$, $k_{sc} \approx 1.06$, and erf is the error function [33,34]. Equation (19) has three structural levels in the square bracket along with a term outside of the square brackets that accounts for the enthalpy of mixing. χ is the Flory-Huggins interaction parameter per Kuhn unit and is based on the zero-conformational-entropy

units, the Kuhn units, rather than the chemical mer units, ϕ is the polymer volume fraction, and $K_v = v_{pol}/v_{sol}$, where v_{pol} and v_{sol} are the segmental volumes of the Kuhn unit and the solvent molecule, respectively. Amongst the three pairs of structural terms in the square brackets, the first term with lead factor of $(f-1)/2$ accounts for the interarm interactions similar to Benoit's second term in Eq. (18). The second term accounts for scattering from the star in the absence of correlations between arms while the third term with subscript p represent the rodlike persistent scaling regime. In each bracket, the first term represents the Guinier exponential decay and the second term yields the power law. $z = G_f/G_p$, is the weight-average number of Kuhn units in the star molecule [31]. K_f and K_p are ratios of the power-law prefactor to the Guinier prefactor for the fractal and persistent regimes. l_p and R_g are the persistence length and the radius of gyration of the fractal star polymer, respectively [32]. It is assumed here that the Kuhn length $l_k = 2l_p$ is the zero-entropy unit [29] for the star. The Guinier prefactor for the fractal regime, G_f, is given by [28]

$$G_f = v_{pol} z \phi N_A (b_{pol} - b_{sol})^2, \tag{20}$$

where b_{pol} and b_{sol} are the scattering length densities of the polymer Kuhn unit and solvent molecule, respectively [28,44]. d_{min} for a monodisperse star is given by [28,31,32,45]

$$d_{min} = \frac{B_f R_g^{d_f}}{G_f \Gamma\left(\frac{d_f}{2}\right)}. \tag{21}$$

Equation (21) is valid for monodisperse samples [32,45]. The second virial coefficient (A_2) is related to Flory χ parameter by [28]

$$A_2 = \frac{\left(\frac{1}{2} - \chi\right)}{V_{pol}\rho_{pol}^2}, \tag{22}$$

where V_{pol} and ρ_{pol} are the molar volume of the solvent and the density of polymer, respectively.

III. MATERIALS AND METHODS

Small-angle neutron scattering was performed on 1 wt% solutions of polyisoprene stars in deuterated p-xylene at 34.5 °C. Deuterated p-xylene was purchased from Cambridge Isotopes. A small amount of 500 ppm of butylhydroxytoluene was added as a stabilizer before addition of the polymer. It was experimentally determined that the solutions were below the overlap concentration. SANS experiments were carried out at the HFIR CG-2 General Purpose SANS facility at Oak Ridge National Laboratory (ORNL) and at the NCNR NG7 SANS facility at the National Institute of Standards and Technology (NIST). At CG-2, SANS experiments were run at sample-to-detector distances of 18.5 and 0.75 m, while at NG7, experiments were done at 15, 7, and 1 m. The low-q data were calibrated with an aluminum standard to obtain absolute intensity.

Two linear standards were purchased from Polymer Standards Service (PSS) GmbH, Mainz, Germany with M_w of (i) 23.6 kg/mole, M_n of 23.3 kg/mole, polydispersity index (PDI) of 1.01 and (ii) 85.4 kg/mole, M_n of 84.2 kg/mole, PDI of 1.01. Other linear, three-arm, four-arm, and six-arm polyisoprene stars were synthesized by anionic/living polymerization utilizing high-vacuum techniques and standard chlorosilane chemistry [46]. In brief, all polymerizations and linking reactions were carried out in evacuated n-Butyllithium(BuLi)-washed and solvent-rinsed glass homemade reactors. Reagents were introduced via break seals and aliquots for characterization were removed by heat sealing of constrictions. First, narrow-molecular-weight-range linear living (active macroanion) polyisoprenes (PIs) were prepared, with sec-BuLi as initiator, in benzene at 25 °C. A small aliquot of the living

TABLE II. Synthesis and characterization details for linear, three-arm, four-arm, and six-arm PI star polymers each with arm molecular weights of ~10.5,38, and 46 kg/mole.

		M_n arm (kg/mol), SEC			Final star-branched PI (SEC-MALS)		$f = M_{n,\text{star}}/M_{n,\text{arm}}$	
Arm	1,4 PI type	Calc.[a]	SEC[b]	M_w/M_n	M_n (kg/mol)	M_w/M_n	Calc.[c]	SEC[d]
10.5k	Linear[a]	23.6	–	1.01	–	–	Linear	–
	3-arm	10	10.5	1.02	30.27	1.02	2.88	3.03
	4-arm	10	10.5	1.02	39.76	1.03	3.79	3.98
	6-arm	10	10.5	1.02	64.05	1.02	6.10	6.41
38k	Linear	74	68	1.01	68.13	1.02	Linear	–
	3-arm	35	38	1.03	101.0	1.01	2.66	2.89
	4-arm	35	38	1.03	133.2	1.01	3.51	1
	6-arm	35	38	1.03	201.4	1.01	5.30	5.75
46k	Linear[b]	85.4	–	1.01	–	–	Linear	–
	3-arm	50	46	1.01	132.7	1.03	2.88	2.65
	4-arm	50	46	1.01	181.7	1.01	3.95	3.63
	6-arm	50	46	1.01	267.7	1.01	5.82	5.35

[a]Purchased from PSS Polymer Standards Service GmbH (M_w of 23.6 kg/mole, M_n of 23.3 kg/mole).
[b]Purchased from PSS Polymer Standards Service GmbH (M_w of 85.4 kg/mole, M_n of 84.2 kg/mole).
[c]Calculated values from chemical stoichiometry.
[d]SEC-MALS-determined values.

PI was removed, terminated with degassed methanol (MeOH), and used for molecular weight characterization (arm of the star). The living polyisoprenyllithium, prior to reaction with the multifunctional chlorosilane compound, was end capped with a few butadiene (Bd) units, in order to increase the living site reactivity. Trichloromethylsilane (CH_3SiCl_3), tetrachlorosilane ($SiCl_4$), and 1,2-bis(trichlorosilyl)ethane (6SiCl) were used as coupling agents for the synthesis of three-, four-, and six-arm star PIs, respectively. About 10% excess of the living end-capped PI to the SiCl, was used in order to force the linking reaction to completion. The excess living chains were terminated with degassed methanol and the final products (star + excess arm) were extensively fractionated (solvent-nonsolvent: toluene-methanol) to remove the arm chains [46].

All intermediates and final products were analyzed by size exclusion chromatography (SEC) and nuclear magnetic resonance (NMR). SEC experiments were carried out at 25 °C with a Waters model 510 pump, a Waters model 410 differential refractometer, and three Styragel columns having a porosity range from 10^3 to 10^6 Å. The carrier solvent was a mixture of chloroform and triethylamine (95/5, v/v) at a flow rate of 1.0 ml/min. Polystyrene standards were used for calibration; the M_n was obtained after applying appropriate correction coefficients. For all arms and stars the polydispersity index was lower than 1.1. The details of the samples are given in Table II. NMR spectra, generated with a Bruker 400-MHz instrument in $CDCl_3$ at 25 °C, revealed that all PIs have a high 1,4 content (93%–94%).

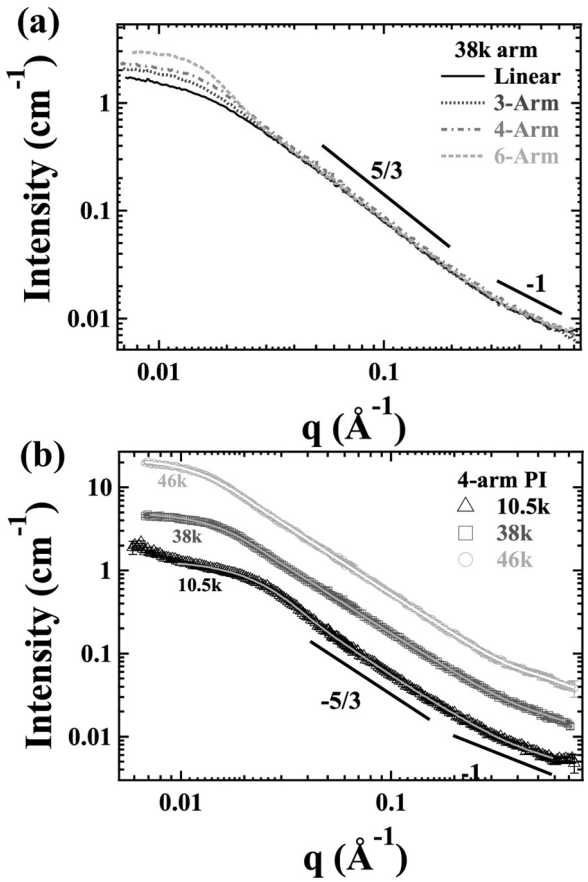

FIG. 2. (a) SANS data from ∼1 wt% 38*k*-arm star polyisoprene polymer solutions in xylene for linear, three-arm, four-arm, and six-arm polymers shown in black and dark gray dots, gray dash-dots, and light gray dashes, respectively. (b) SANS from a solution of ∼1 wt% for four-arm star polyisoprene in xylene for 10.5*k*, 38*k*, and 46*k* arms in black triangles, dark gray squares, and light gray circles with respective Hybrid Unified Fits [Eq. (19)] in solid contrast lines. The data and their respective fits are offset for visual clarification. Slopes of −5/3 and −1 are also shown for reference.

IV. RESULTS AND DISCUSSION

The distinguishing feature of the SANS data on all samples is a power-law decay of slope close to −5/3, reflecting a mass fractal dimension of 5/3 following the prediction of Eq (8), as shown in Fig. 2. In addition to this feature a prominent knee is observed at low q,reflecting correlations between the star arms. The effect of arm length can be seen in Fig. 2(b) where the knee shifts towards lower q for higher arm molecular weights. The "*k*" in figure legends and discussion indicates kg/mole for each arm of the star polymers. Equation (19) was used to fit the experimental curves for the star samples listed in Table II, also shown for four-arm stars in Fig. 2(b). The fitting and evaluated scaling parameters from the hybrid unified fit are tabulated in Table III.

For constant arm length, both z and R_g increase with increase in functionality, as shown in Figs. 3(a) and 3(b). The persistence length l_p varies in the range of ∼12.5 ± 1.5 Å except for the linear sample for the 38*k* series. z, R_g, and l_p all are somewhat higher for this sample.

The χ parameter was constant within error limits at ∼0.22 ± 0.04, shown in Fig. 4(a). This agrees rather well with the reported values of 0.27 in the literature [47,48]. It should be pointed out that the χ parameter evaluated here is based on the zero-entropy Kuhn unit rather than the chemical mer unit. The second virial coefficient A_2 shown in Fig. 4(b) has a value of ∼0.0026 ± 0.0004 mol cm^3/g^2. None of these local enthalpic parameters are affected by the functionality or molecular weight of the star polymers.

The data show a rather constant fractal dimension d_f, close to 5/3 across all sets of samples [Fig. 5(a)], consistent with Eq. (8). The natural tendency for the structures to equilibrate to $d_f = 5/3$ is remarkable, supporting the modified Flory-Krigbaum prediction. The connectivity dimension c, shown in Fig. 5(b), is bound by Eq. (12) to the functionality f and z. Therefore differences between the three sets of samples with the same functionality reflect the effect of mass alone. Figure 5(b) also shows that c is high for short-armed stars which is consistent with Eq. (13). $d_{\min}$ [Fig. 5(c)] is a conjugate parameter reflecting the average tortuosity in the structure. The decrease in tortuosity with functionality indicates that the arms straighten out as functionality increases, maintaining a constant mass fractal dimension. As c is high for short-armed stars, $d_{\min}$ actually decreases since the overall mass density remains constant. It essentially means that, at an average, the arms of stars with higher mass are comparatively more tortuous.

The minimum path p is the number of Kuhn units from one side of the star to the other, so two arm lengths, Fig. 6(a).

TABLE III. Fitted, thermodynamic, and calculated scaling parameters for PI polymer samples using the unified fit function Eq. (19).

Arm MW	f	R_g (Å)	z	d_f	χ[a]	$10^3 A_2$ (mol cm^3 g^{-2})	l_p (Å)	$d_{\min}$	c	p	s	ϕ_{Br}[b]	ϕ_M	ϕ_{Si}
10.5k	Linear	44.6 ± 0.2	19 ± 1	1.67 ± 0.02	0.22 ± 0.03	2.7 ± 0.3	12.5 ± 0.1	1.67 ± 0.07	1.00 ± 0.05	19.0 ± 0.6	5.8 ± 0.5	0.0 ± 0.0	0.69 ± 0.06	0.0 ± 0.0
	3	62 ± 1	34 ± 1	1.67 ± 0.01	0.21 ± 0.03	2.8 ± 0.3	11.8 ± 0.8	1.47 ± 0.04	1.13 ± 0.04	22.5 ± 0.4	11 ± 1	0.33 ± 0.05	0.67 ± 0.08	0.104 ± 0.006
	4	67 ± 2	44 ± 2	1.69 ± 0.02	0.19 ± 0.03	3.0 ± 0.3	13.3 ± 0.4	1.4 ± 0.1	1.2 ± 0.1	22.0 ± 0.8	16 ± 4	0.5 ± 0.1	0.6 ± 0.1	0.17 ± 0.02
	6	68 ± 2	61 ± 4	1.66 ± 0.01	0.18 ± 0.03	3.1 ± 0.3	12.2 ± 0.3	1.2 ± 0.1	1.4 ± 0.1	20.4 ± 0.8	30 ± 10	0.7 ± 0.2	0.5 ± 0.2	0.36 ± 0.06
38k	Linear	110 ± 7	80 ± 1	1.75 ± 0.04	0.36 ± 0.02	2.7 ± 0.3	16.6 ± 0.2	1.75 ± 0.07	1.00 ± 0.07	80 ± 1	12.2 ± 0.1	0.0 ± 0.0	0.85 ± 0.09	0.0 ± 0.0
	3	114 ± 2	104 ± 2	1.66 ± 0.02	0.20 ± 0.02	2.8 ± 0.3	12.9 ± 0.2	1.52 ± 0.06	1.10 ± 0.06	69 ± 1	21.4 ± 0.3	0.33 ± 0.08	0.79 ± 0.09	0.059 ± 0.003
	4	119 ± 3	148 ± 1	1.66 ± 0.01	0.19 ± 0.03	3.0 ± 0.3	11.4 ± 0.2	1.43 ± 0.03	1.16 ± 0.03	74.1 ± 0.6	32.9 ± 0.2	0.50 ± 0.07	0.78 ± 0.06	0.101 ± 0.003
	6	133 ± 5	202 ± 3	1.66 ± 0.02	0.22 ± 0.03	3.1 ± 0.3	11.7 ± 0.2	1.32 ± 0.04	1.26 ± 0.05	67.4 ± 0.7	56.3 ± 0.6	0.7 ± 0.1	0.72 ± 0.09	0.181 ± 0.007
46k	Linear	112 ± 1	98 ± 3	1.67 ± 0.07	0.17 ± 0.04	3.2 ± 0.4	11.1 ± 0.2	1.7 ± 0.1	1.00 ± 0.05	98 ± 3	15.5 ± 0.3	0.0 ± 0.0	0.84 ± 0.06	0.0 ± 0.0
	3	138 ± 6	155 ± 2	1.66 ± 0.06	0.25 ± 0.09	2.4 ± 0.9	13.4 ± 0.1	1.53 ± 0.08	1.09 ± 0.09	104 ± 2	27.0 ± 0.3	0.3 ± 0.1	0.83 ± 0.08	0.049 ± 0.002
	4	144 ± 6	201 ± 4	1.67 ± 0.04	0.24 ± 0.02	2.5 ± 0.2	13.1 ± 0.6	1.45 ± 0.06	1.15 ± 0.08	101 ± 2	39.1 ± 0.5	0.5 ± 0.2	0.81 ± 0.1	0.085 ± 0.005
	6	160 ± 10	293 ± 3	1.68 ± 0.05	0.23 ± 0.03	2.7 ± 0.2	12.4 ± 0.2	1.36 ± 0.06	1.24 ± 0.09	98 ± 1	65.3 ± 0.5	0.7 ± 0.2	0.78 ± 0.2	0.135 ± 0.004

[a]χ determined per Kuhn unit.
[b]Bound by Eq. (8).

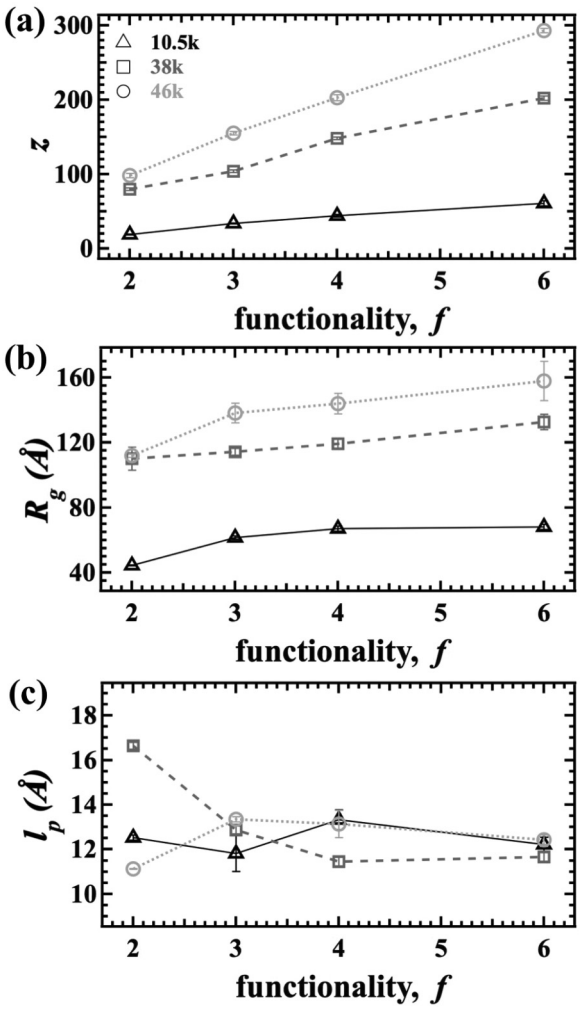

FIG. 3. (a) Mass z, (b) radius of gyration, R_g, and (c) persistent lengths l_p as functions of functionality f.

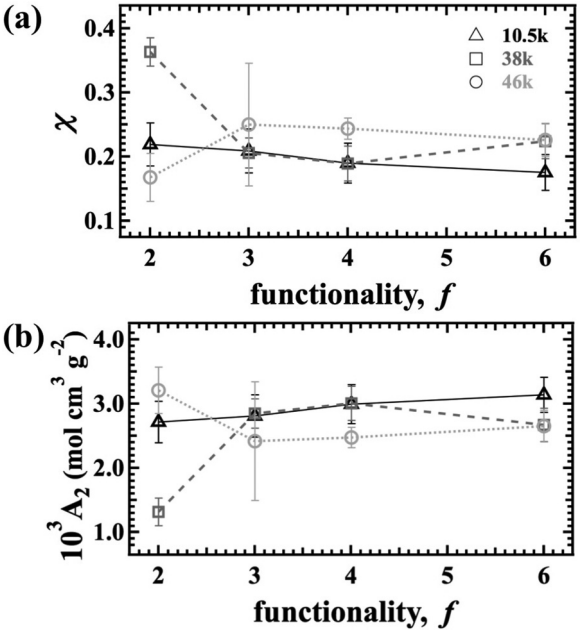

FIG. 4. (a) Flory-Huggins interaction parameter χ and (b) second virial coefficient A_2 as functions of functionality f.

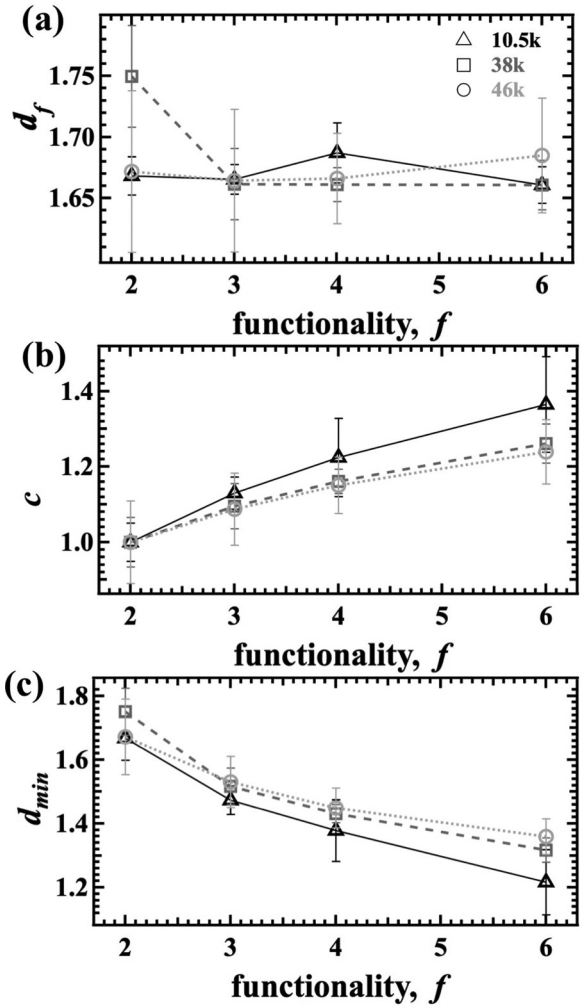

FIG. 5. (a) Fractal dimension d_f, (b) connectivity dimension c, and (c) minimum dimension $d_{\min}$ as functions of functionality f.

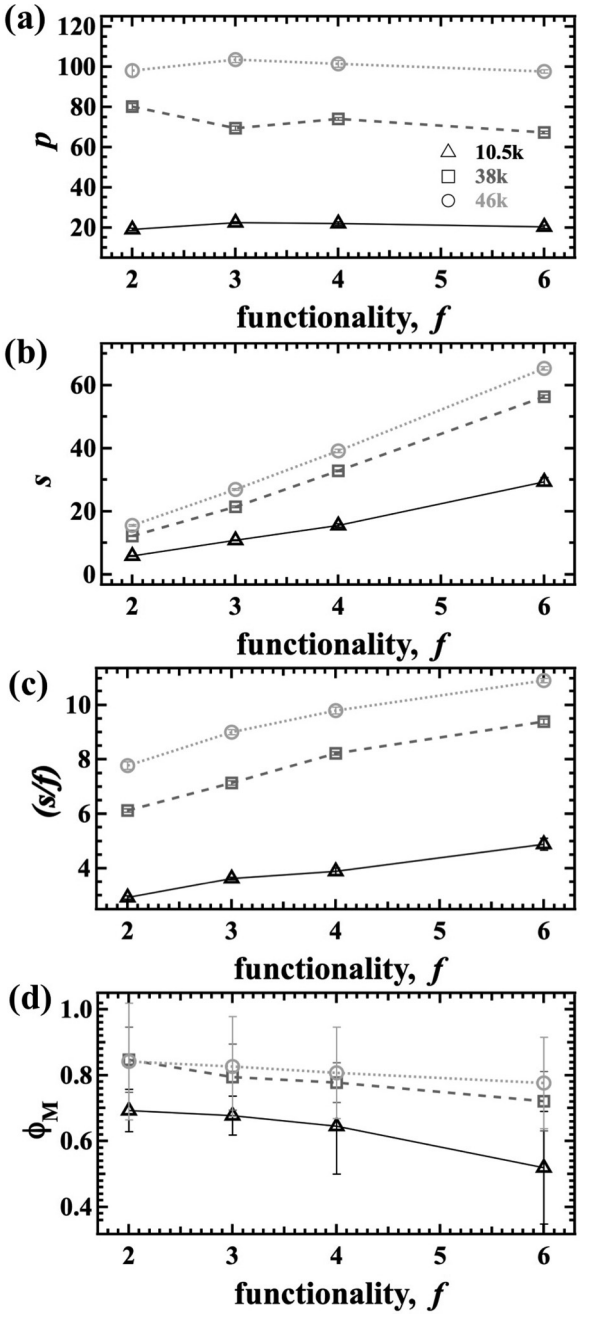

FIG. 6. (a) Minimum path p, (b) connectivity path s, (c) s/f, and (d) meandering mole fraction (ϕ_M) as functions of functionality f.

This remains constant with functionality for a fixed arm mass, as anticipated. The connective path s quantifies the mass of a stick figure structure connecting end points and the core in terms of the number of Kuhn units, shown in Fig. 6(b). When normalized by the number of arms, s/f, it can be clearly seen that the arms straighten out with increasing functionality, as shown in Fig. 6(c). s increases with functionality due to straightening of the arms. s also increases with the mass of the arms. The meandering mole fraction ϕ_M, which is the fraction of the chain that accounts for mass that is not used in linear (stick figure) connectivity, can be evaluated using Eq. (9). ϕ_M decreases with increase in functionality, as shown in Fig. 6(d), indicating that the arms become less convoluted with increasing functionality.

The monomer density of the chain is a function of the mass, $\rho = z^{1-1/d_f}$. The stars display constant mass fractal dimension according to Eq. (8). Since the mass fractal dimension is constant, there is no significant change in local density as a function of radial position in the star, as was predicted by the DC model. Rather, the stars behave similar to the Benoit fractal model, but with good-solvent scaling. The radially varying feature of the star structure is an increase in chain tortuosity with distance from the core rather than the density gradient assumed in the DC model. The radial increase in tortuosity allows for a constant radial density profile.

The scaling parameters consistently point toward straightening of the arms with functionality, shown in Fig. 5. The local mass density, reflected in the mass fractal dimension, remains the same, Fig. 5(a), while the minimum dimension decays with functionality, indicating a reduction in tortuosity with functionality. Such a steric phenomenon can be quantified using Eq. (15). $\phi_{\rm Si}$ is a mole fraction quantifying steric effects and shown in Fig. 7(a). Steric effects are greater at higher functionalities and lower arm molecular weights. $\phi_{\rm Si}$ values for the six-arm stars rise to 0.36 ± 0.06, 0.181 ± 0.007, and

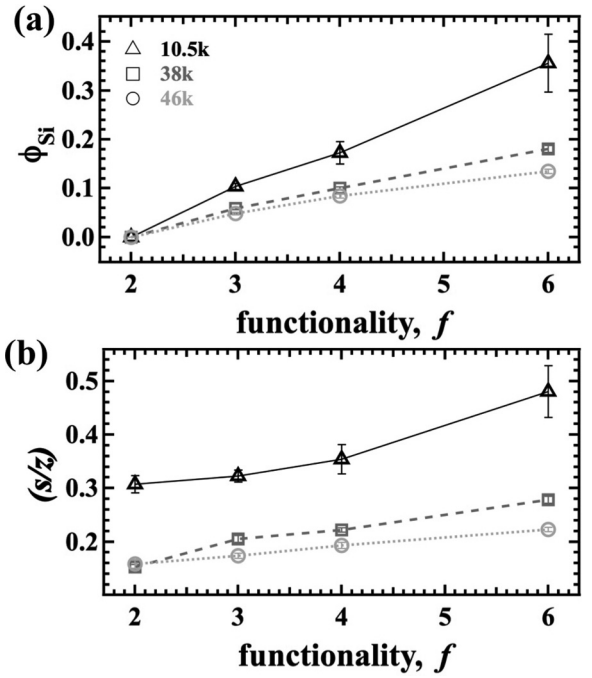

FIG. 7. (a) ϕ_{Si}, and (b) s/z as functions of functionality f.

0.135 ± 0.004 for $10.5k-$,$38k-$, and $46k$-arm stars respectively. The corresponding ϕ_{Si} for four-arm stars are $0.17 \pm 0.02, 0.101 \pm 0.001$, and 0.085 ± 0.005 and those for three-arm stars are $0.104 \pm 0.006, 0.059 \pm 0.003$, and 0.049 ± 0.002. ϕ_{Si} for the six-arm $10.5k$ sample is about 36% of a fully extended arm structure!

Figure 8 is a schematic, projected in two dimensions (2D) for clarity, summarizing the scaling parameters considered in the present investigation. The local mass density of the structure remains radially the same. In order to accommodate an increase in conical volume with radius, the chain becomes more tortuous. The results may be compared and contrasted with the Daoud and Cotton model where the local density is predicted to decrease with radial position away from the center. The DC model predicts three regimes based on relationships between density, f, and z. In contrast, the modified Flory-Krigbam approach and results shown here predict that the density is given by $\phi(r) \sim (r/l)^{-4/\beta}$ irrespective of distance from the core.

V. CONCLUSION

Molecular topology generally has a direct influence on the mass fractal dimension and other scaling dimensions for fractal structures. In this paper it is shown that polymers at thermal equilibrium are a distinct class of fractals where the mass fractal dimension is not affected by chain topology. The consequence of this is chain straightening with increasing chain complexity. A theoretical basis for this observation comes from a slight modification to the Flory-Krigbaum theory.

The chain scaling dimensions and interaction parameter of star topologies were obtained using a Hybrid Unified scattering function that accounts for interarm correlations in symmetric star polymers along with the polymer-solvent interaction parameter for chains of arbitrary scaling dimension. The structural and thermodynamic parameters for different molecular weights and functionality polyisoprene stars were considered under good solvent conditions.

The results were compared and contrasted with the Daoud and Cotton model where equal segments of the arms are confined to blobs of radially increasing size, which can fit within a cone, leading to a radially decreasing chain density. Our results contradicted the presumption that a radial density gradient exists. The results demonstrate the ability of star topologies to redistribute the mass through changes in chain tortuosity such that the mass fractal dimension remains constant throughout the structure and for stars of different functionality.

For symmetric star polymers the branch fraction ϕ_{Br} can be directly calculated from the star functionality, leading to a verification of the structure. Our results quantify steric effects in symmetric stars and show that steric straightening in star polymers is more significant for lower-molecular-weight arms and stars with higher functionalities. A modification of the

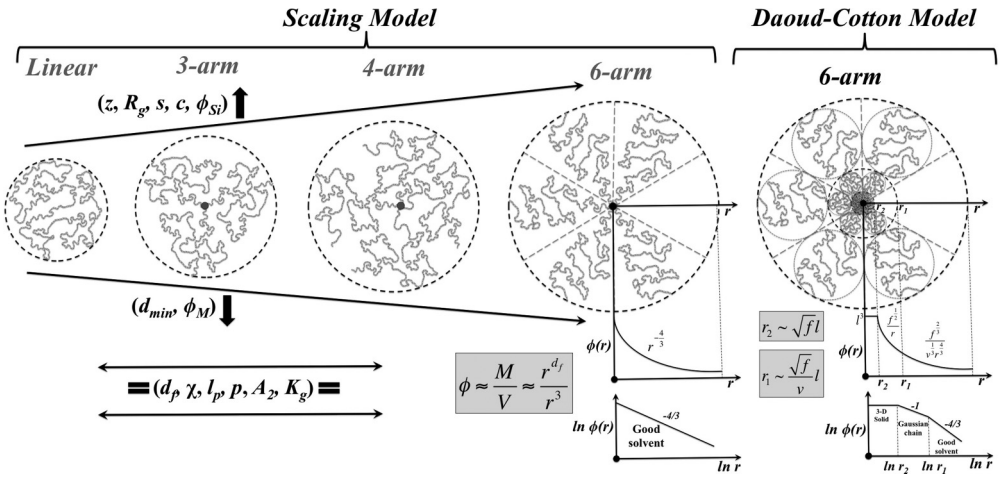

FIG. 8. Schematic demonstrating changes in scaling and thermodynamic parameters with functionality for the same arm length. The scaling model for the six-arm star polymer is compared with that of the Daoud-Cotton model [13]. l and v are the monomer length and excluded volume associated with each monomer.

Flory and Krigbaum theory showed that the size of stars depends on the mass, functionality, and Kuhn length with a similar dependence to that of the DC model except that the dependence on Kuhn length is slightly different.

ACKNOWLEDGMENTS

R.K. and N.H. thank Dr. Ema Zagar, National Institute of Chemistry Slovenia, for the SEC-MALS characterization of the star PIs. The research conducted at ORNL's High Flux Isotope Reactor was sponsored by the Scientific User Facilities Division, Office of Basic Energy Sciences, U.S. Department of Energy (USA). We acknowledge the support of the National Institute of Standards and Technology (USA), U.S. Department of Commerce, in providing the neutron research facilities used in this work. D.K.R. is supported by the Laboratory Directed Research and Development Program of Oak Ridge National Laboratory.

[1] J. R. Schaefgen and P. J. Flory, Synthesis of multichain polymers and investigation of their viscosities, J. Am. Chem. Soc. **70**, 2709 (1948).
[2] J. M. Desimone, Branching out into new polymer markets, Science **269**, 1060 (1995).
[3] C. Mayer, E. Zaccarelli, E. Stiakakis, C. N. Likos, F. Sciortino, A. Munam, M. Gauthier, N. Hadjichristidis, H. Iatrou, P. Tartaglia, H. Lowen, and D. Vlassopoulos, Asymmetric caging in soft colloidal mixtures, Nat. Mater. **7**, 780 (2008).
[4] M. Watzlawek, C. N. Likos, and H. Lowen, Phase Diagram of Star Polymer Solutions, Phys. Rev. Lett. **82**, 5289 (1999).
[5] G. Widawski, M. Rawiso, and B. Francois, Self-organized honeycomb morphology of star-polymer polystyrene films, Nature (London) **369**, 387 (1994).
[6] D. K. Bick and T. C. B. McLeish, Topological Contributions to Nonlinear Elasticity in Branched Polymers, Phys. Rev. Lett. **76**, 2587 (1996).
[7] S. T. Milner and T. C. B. McLeish, Reptation and Contour-Length Fluctuations in Melts of Linear Polymers, Phys. Rev. Lett. **81**, 725 (1998).
[8] N. Hadjichristidis, M. Pitsikalis, S. Pispas, and H. Iatrou, Polymers with complex architecture by living anionic polymerization, Chem. Rev. **101**, 3747 (2001).
[9] J. Batoulis and K. Kremer, Thermodynamic properties of star polymers–good solvents, Macromolecules **22**, 4277 (1989).
[10] J. Roovers, P. M. Toporowski, and J. Douglas, Thermodynamic properties of dilute and semidilute solutions of regular star polymers, Macromolecules **28**, 7064 (1995).
[11] B. H. Zimm and W. H. Stockmayer, The dimensions of chain molecules containing branches and rings, J. Chem. Phys. **17**, 1301 (1949).
[12] G. S. Grest, L. J. Fetters, J. S. Huang, and D. Richter, Star polymers: Experiment, theory, and simulation, Adv. Chem. Phys. **94**, 67 1996).
[13] M. Daoud and J. P. Cotton, Star shaped polymers—A model for the conformation and its concentration-dependence, J. Phys. **43**, 531 (1982).
[14] T. M. Birshtein and E. B. Zhulina, Conformations of star-branched macromolecules, Polymer **25**, 1453 (1984).
[15] W. D. Dozier, J. S. Huang, and L. J. Fetters, Colloidal nature of star polymer dilute and semidilute solutions, Macromolecules **24**, 2810 (1991).
[16] P. M. Wood-Adams, J. M. Dealy, A. W. deGroot, and O. D. Redwine, Effect of molecular structure on the linear viscoelastic behavior of polyethylene, Macromolecules **33**, 7489 (2000).
[17] R. Everaers, S. K. Sukumaran, G. S. Grest, C. Svaneborg, A. Sivasubramanian, and K. Kremer, Rheology and microscopic topology of entangled polymeric liquids, Science **303**, 823 (2004).
[18] L. J. Fetters, A. D. Kiss, D. S. Pearson, G. F. Quack, and F. J. Vitus, Rheological behavior of star-shaped polymers, Macromolecules **26**, 647 (1993).
[19] A. T. Boothroyd and R. C. Ball, Conformation of star polymers without excluded volume, Macromolecules **23**, 1729 (1990).
[20] P. G. De Gennes, *Scaling Concepts in Polymer Physics* (Cornell University Press, New York, 1979).
[21] H. Benoit, On the effect of branching and polydispersity on the angular distribution of the light scattered by Gaussian coils, J. Polym. Sci. **11**, 507 (1953).
[22] J. S. Pedersen, Analysis of small-angle scattering data from colloids and polymer solutions: Modeling and least-squares fitting, Adv. Colloid Interface Sci. **70**, 171 (1997).
[23] F. Candau, P. Rempp, and H. Benoit, A new theoretical approach to the problem of solution behavior of branched polymers, Macromolecules **5**, 627 (1972).
[24] T. A. Orofino, Branched polymers. Ii—dimensions in non-interacting media, Polymer **2**, 305 (1961).
[25] P. J. Flory and J. G. Jackson, *Statistical Mechanics of Chain Molecules* (Hanser, Cincinnati, 1989).
[26] W. R. Krigbaum and P. J. Flory, Statistical mechanics of dilute polymer solutions. III. Ternary mixtures of 2 polymers and a solvent, J. Chem. Phys. **20**, 873 (1952).
[27] W. R. Krigbaum and P. J. Flory, Statistical mechanics of dilute polymer solutions. V. Evaluation of thermodynamic interaction parameters from dilute solution measurements, J. Am. Chem. Soc. **75**, 5254 (1953).
[28] D. K. Rai, G. Beaucage, K. Ratkanthwar, P. Beaucage, R. Ramachandran, and N. Hadjichristidis, Determination of the interaction parameter and topological scaling features of symmetric star polymers in dilute solution, Phys. Rev. E **92**, 012602 (2015).
[29] W. Kuhn, Über die Gestalt Fadenförmiger Moleküle in Lösungen, Kolloidn. Z. **68**, 2 (1934).
[30] G. Beaucage and A. S. Kulkarni, Dimensional description of cyclic macromolecules, Macromolecules **43**, 532 (2010).
[31] G. Beaucage, Determination of branch fraction and minimum dimension of mass-fractal aggregates, Phys. Rev. E **70**, 031401 (2004).
[32] R. Ramachandran, G. Beaucage, A. S. Kulkarni, D. McFaddin, J. Merrick-Mack, and V. Galiatsatos, Persistence length of short-chain branched polyethylene, Macromolecules **41**, 9802 (2008).

[33] G. Beaucage, Approximations leading to a unified exponential power-law approach to small-angle scattering, J. Appl. Crystallogr. **28**, 717 (1995).

[34] G. Beaucage, Small-angle scattering from polymeric mass fractals of arbitrary mass-fractal dimension, J. Appl. Crystallogr. **29**, 134 (1996).

[35] R. Ramachandran, G. Beaucage, D. K. Rai, D. J. Lohse, T. Sun, A. H. Tsou, A. Norman, and N. Hadjichristidis, Quantification of branching in model three-arm star polyethylene, Macromolecules **45**, 1056 (2012).

[36] D. K. Rai, G. Beaucage, E. O. Jonah, D. T. Britton, S. Sukumaran, S. Chopra, G. G. Gonfa, and M. Harting, Quantitative investigations of aggregate systems, J. Chem. Phys. **137**, 044311 (2012).

[37] D. K. Rai, Quantification of fractal systems using small angle scattering, Doctoral dissertation, University of Cincinnati, 2013.

[38] D. Anunciado, D. Rai, S. Qian, V. Urban, and H. O'Neill, Small-angle neutron scattering reveals the assembly of alpha-synuclein in lipid membranes, Biochim. Biophys. Acta: Proteins Proteomics **1854**, 1881 (2015).

[39] J. Teixeira, Small-angle scattering by fractal systems, J. Appl. Crystallogr. **21**, 781 (1988).

[40] U. S. Jeng, T. L. Lin, L. Y. Wang, L. Y. Chiang, D. L. Ho, and C. C. Han, SANS structural characterization of fullerenol-derived star polymers in solutions, Appl. Phys. A: Mater. Sci. Process. **74**, S487 (2002).

[41] S. K. Sinha, T. Freltoft, and J. Kjems, Observation of power-law correlations in silica-particle aggregates by small-angle neutron scattering, in *Kinetics of Aggregation and Gelation*, edited by F. Family and D. P. Landau (North-Holland, Amsterdam, 1984), p. 87.

[42] P. Debye and A. M. Bueche, Scattering by an inhomogeneous solid, J. Appl. Phys. **20**, 518 (1949).

[43] A. T. Boothroyd, G. L. Squires, L. J. Fetters, A. R. Rennie, J. C. Horton, and A. Devallera, Small-angle neutron-scattering from star-branched polymers in dilute-solution, Macromolecules **22**, 3130 (1989).

[44] G. Beaucage and R. S. Stein, Tacticity effects on polymer blend miscibility. 3. Neutron scattering analysis, Macromolecules **26**, 1617 (1993).

[45] R. Ramachandran, G. Beaucage, A. S. Kulkarni, D. McFaddin, J. Merrick-Mack, and V. Galiatsatos, Branch content of metallocene polyethylene, Macromolecules **42**, 4746 (2009).

[46] N. Hadjichristidis, H. Iatrou, S. Pispas, and M. Pitsikalis, Anionic polymerization: High vacuum techniques, J. Polym. Sci., Part A: Polym. Chem. **38**, 3211 (2000).

[47] Y. B. Tewari and H. P. Schreiber, Thermodynamic interactions in polymer systems by gas-liquid chromatography. II. Rubber-hydrocarbons, Macromolecules **5**, 329 (1972).

[48] J. E. Mark, *Physical Properties of Polymers* (Cambridge University Press, Cambridge, 2004).